Azimuthal Dependence of Collective Expansion for Symmetric Heavy-Ion Collisions

G. Stoicea,[1] M. Petrovici,[1,4] A. Andronic,[1,4] N. Herrmann,[6] J. P. Alard,[3] Z. Basrak,[11] V. Barret,[3] N. Bastid,[3] R. Čaplar,[11] P. Crochet,[3] P. Dupieux,[3] M. Dželalija,[11] Z. Fodor,[2] O. Hartmann,[4] K. D. Hildenbrand,[4] B. Hong,[9] J. Kecskemeti,[2] Y. J. Kim,[9] M. Kirejczyk,[12] M. Korolija,[11] R. Kotte,[5] T. Kress,[4] A. Lebedev,[7] Y. Leifels,[4] X. Lopez,[3] M. Merschmeier,[6] W. Neubert,[5] D. Pelte,[6] F. Rami,[10] W. Reisdorf,[4] D. Schüll,[4] Z. Seres,[2] B. Sikora,[12] K. S. Sim,[9] V. Simion,[1] K. Siwek-Wilczyńska,[12] V. Smolyankin,[7] M. Stockmeier,[6] K. Wiśniewski,[4] D. Wohlfarth,[5] I. Yushmanov,[8] and A. Zhilin[7]

(FOPI Collaboration)

[1]*National Institute for Nuclear Physics and Engineering, Bucharest, Romania*
[2]*Central Research Institute for Physics, Budapest, Hungary*
[3]*Laboratoire de Physique Corpusculaire, IN2P3/CNRS, and Université Blaise Pascal, Clermont-Ferrand, France*
[4]*Gesellschaft für Schwerionenforschung, Darmstadt, Germany*
[5]*Forschungszentrum Rossendorf, Dresden, Germany*
[6]*Physikalisches Institut der Universität Heidelberg, Heidelberg, Germany*
[7]*Institute for Theoretical and Experimental Physics, Moscow, Russia*
[8]*Kurchatov Institute, Moscow, Russia*
[9]*Korea University, Seoul, South Korea*
[10]*Institut de Recherches Subatomiques, IN2P3-CNRS, Université Louis Pasteur, Strasbourg, France*
[11]*Rudjer Boskovic Institute, Zagreb, Croatia*
[12]*Institute of Experimental Physics, Warsaw University, Poland*

P. Danielewicz[13,14]

[13]*Michigan State University, East Lansing, Michigan 48824, USA*
[14]*Gesellschaft für Schwerionenforschung, Darmstadt, Germany*
(Received 24 February 2003; published 20 February 2004)

Detailed studies of the azimuthal dependence of the mean fragment and flow energies in the Au + Au and Xe + CsI systems are reported as a function of incident energy and centrality. Comparisons between data and model calculations show that the flow energy values along different azimuthal directions could be viewed as snapshots of the fireball expansion with different exposure times. For the same number of participating nucleons more transversally elongated participant shapes from the heavier system produce less collective transverse energy. Good agreement with Boltzmann-Uehling-Uhlenbeck calculations is obtained for a soft nuclear equation of state.

DOI: 10.1103/PhysRevLett.92.072303 PACS numbers: 25.75.Ld, 25.70.Pq

One of the main motivations to study heavy ion collisions at high energy is to obtain information on the equation of state (EOS) for nuclear matter under conditions of pressure and temperature different from those in normal nuclei. The search for hot and dense nuclear matter created in such collisions is confronted with dynamical consequences of the high incident energy necessary to reach such conditions and with the difficulty to reach a thermal equilibrium in finite systems. Dynamical aspects refer not only to the initial phase of the collision, but also to the evolution stage of the formed fireball. Thus, detailed experimental information on the expansion dynamics is required. The simplest situation corresponds to central collisions with the advantage of the azimuthal symmetry and of the lack of spectator matter. Predicted in the early 1970s [1,2], the collective expansion of the hot and dense fireball produced in central collisions was evidenced experimentally [3–11]. Although central collisions seem to deliver the cleanest signal on the collective expansion on first sight, two issues are worth mentioning: (i) While the axial symmetry of the dynamical evolution holds, the spherical symmetry has to be inspected. Preequilibrium emission and transparency effects could influence the spherical symmetry of the expanding system. (ii) With regard to reaching pressure, the nuclear matter, not being confined in transverse directions, can escape freely in any direction perpendicular to the collision axis starting from the very first moments of the collision. For reduced centrality, other complications appear. One has to deal with rotating expanding objects in the presence of spectator matter. Nevertheless, there are also some advantages in studying less central collisions: (i) Rotation and shadowing can be used as internal clocks for getting deeper information on the expansion dynamics; (ii) the centrality can be used to control the shape and content of the fireball and of the shadowing matter; (iii) for a given centrality the passage time of the shadowing objects can be controlled varying the incident

energy; (iv) the confinement of the spectators becomes more efficient in transverse directions than in the central collisions. Symmetry considerations imply two dominant components in the particle transverse emission: azimuthally symmetric emission and an elliptic modulation of that emission (squeeze-out) which has been predicted by hydrodynamical calculations [12] and extensively studied experimentally [13–24]. The squeeze-out has been studied, in particular, as a function of centrality, type of emitted particle, transverse momentum, and mass of the colliding systems. A considerable collectivity was identified in the transverse emission pattern and it was found, from fitting the energy spectra with a radially expanding source, that the collectivity itself exhibits an elliptic modulation [19]. The present Letter is devoted to the elliptic modulation of collectivity as reflected in the dependence of average fragment energies on the fragment mass [22].

Notably, without any modulation of collectivity, the squeeze-out itself could just represent pure geometric shadowing of particle emission from the participant zone. Significant modulations, as a counterpart, should show significant influence by early pressure, with the compression and excitation energy getting converted into collective energy at the stage of high density when the spectators are present. Comparisons of different centralities and system masses are needed in order to understand how the geometry of the participant and spectator zones affects the collective expansion. Excitation functions for the collectivity anisotropy are mandatory to understand how the collective expansion builds up at different densities and excitations.

The present work is based on ^{197}Au + ^{197}Au and ^{130}Xe + ^{133}Cs^{127}I data from FOPI Phase II experiments at the SIS of GSI. Detector details can be found elsewhere [24–26]. The main component implemented in the FOPI configuration is a central drift chamber (CDC) [26]. Two criteria for centrality selection were combined: the particle multiplicity, with a higher selectivity at large impact parameters, and the ratio of transverse and longitudinal energies in the c.m. system $E_{\rm rat} = \sum_i E_{\perp,i}/\sum_i E_{\parallel,i}$, as a better filter for more central collisions. Two windows in the CDC multiplicity, CM2 and CM3, have been used to select impact parameters in the range of 6–8 fm and 4–6 fm. Similarly, the ER4 and ER5 windows in $E_{\rm rat}$ select the ranges 2–4 fm and 0–2 fm, respectively. The impact parameter estimates and the estimates of the number of participating nucleons $A_{\rm part}$ are based on the geometrical "sharp cutoff" approximation. For reaction-plane determination, the transverse-momentum analysis method has been used [27]. Studies of the squeeze-out phenomena revealed from the very beginning [13] the importance of performing the azimuthal distribution analysis in a reference frame with the polar axis along the sidewards flow direction. The present analysis used a reference frame in which the ellipsoidal pattern of the azimuthal particle distribution at midrapidity maximizes the ratio of the two transverse semiaxes [19,22,24]. The previous comprehensive description of the elliptic modulation of collectivity in the beam range 0.25–1.15A GeV [19] was based on a parametrization of the deuteron ($A = 2$) tranverse-mass spectra with an expression characteristic of radially symmetric shell expansion. The use of such an expression for studying the modulations is inherently contradictory and implies a specific model. We prefer to present experimental information free from any model.

For the mentioned reasons, we concentrate on the mean kinetic energy in the c.m. system, $\langle E_{\rm kin}^{\rm c.m.}\rangle$, and on the flow energy extracted from its dependence on the mass of the reaction products ($Z = 1$, 2, and 3) within a polar angular range of $80° \le \theta_{\rm c.m.} \le 100°$ [22]. In order to extract $\langle E_{\rm kin}^{\rm c.m.}\rangle$, one needs complete energy spectra. Because of the peculiar shape of the shadows of subdetector borders in the rotated reference frame, the experimental spectra have been analyzed in the azimuthal ranges [0°, 90°] and [270°, 360°]. These two ranges have been overlapped to decrease statistical errors. They are plotted as full symbols in Fig. 1 for five bins from 0° to 90° and were then reflected (open symbols) in order to generate the full angular range of 0°–360°.

Figure 1 presents, as an example, the azimuthal dependence of $\langle E_{\rm kin}^{\rm c.m.}\rangle$ for $Z = 2$ products as a function of the incident energy in Au + Au at ER4 centrality, as a function of centrality in Au + Au at 250A MeV, and for the two measured systems at 250A MeV and ER4 centrality. The presented information is *independent* of the anisotropy of the yield distribution. The main contribution to the error bars comes from systematic effects, the statistical ones being at the level of symbol sizes. We had to combine information from two subdetector systems and this was done by looking at all fragments as a function of

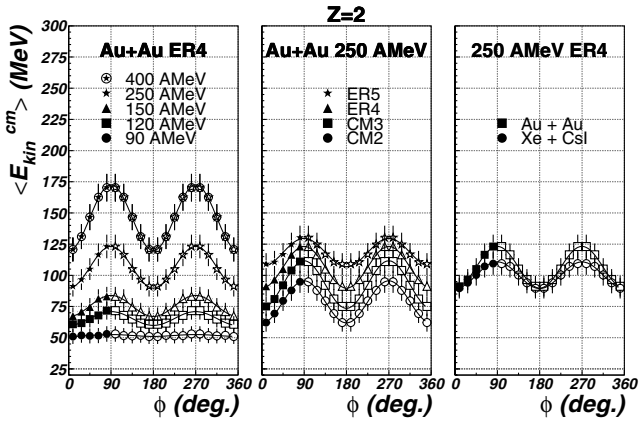

FIG. 1. Mean c.m. energy $\langle E_{\rm kin}^{\rm c.m.}\rangle$ of $Z = 2$ products as a function of the azimuthal angle, shown for Au + Au at ER4 centrality and different energies (left); Au + Au at 250A MeV and different centralities (middle); Au + Au and Xe + CsI at 250A MeV and ER4 centrality (right). The error bars include systematic effects.

their charge. In doing this, we had to correct the $Z = 1$ and $Z = 2$ energy spectra from the CDC, based on previous FOPI data [8], in order to take into account the fact that the ^{3}He fragments are not well separated from the tritons in some parts of the momentum space. The azimuthal asymmetry of $\langle E_{\rm kin}^{\rm c.m.}\rangle$ increases as a function of incident energy and mass of the colliding nuclei, reaching a maximum in midcentral collisions. The value averaged over the azimuth increases with the beam energy, centrality, and mass of interacting system. As shown by the solid lines, the data follow very well the behavior $\langle E_{\rm kin}^{\rm c.m.}\rangle = E_{\rm kin}^0 - \Delta E_{\rm kin}\cos 2\Phi$. Fits to the dependence of mean kinetic energies $\langle E_{\rm kin}^{\rm c.m.}\rangle$ on fragment mass A with the nonrelativistic expression

$$\langle E_{\rm kin}^{\rm c.m.}\rangle \approx \tfrac{1}{2}A \cdot m_0\langle\beta_{\rm flow}^2\rangle + \tfrac{3}{2}T, \qquad (1)$$

yield the average flow energy per nucleon $E_{\rm coll}$ and the temperature T (m_0 is the nucleon rest mass). Lack of an explicit treatment of the Coulomb effects leads to a systematically overestimated value of the real temperature T [8].

The flow energy $E_{\rm coll} = \frac{1}{2}m_0\langle\beta_{\rm flow}^2\rangle$ and T can be fit nicely with $E_{\rm coll} = E_{\rm coll}^0 - \Delta E_{\rm coll}\cos 2\Phi$ and $T = T_0 - \Delta T\cos 2\Phi$, respectively. $E_{\rm coll}$ exhibits a strong elliptic anisotropy, with the largest energy values in the direction perpendicular to the reaction plane. Both the average over the azimuth of the collective energy $E_{\rm coll}^0$ and the elliptic anisotropy $\Delta E_{\rm coll}$ increase continuously with the incident energy over the studied region. The temperature parameter T stays roughly constant as a function of the azimuth at three lowest beam energies and develops oscillations

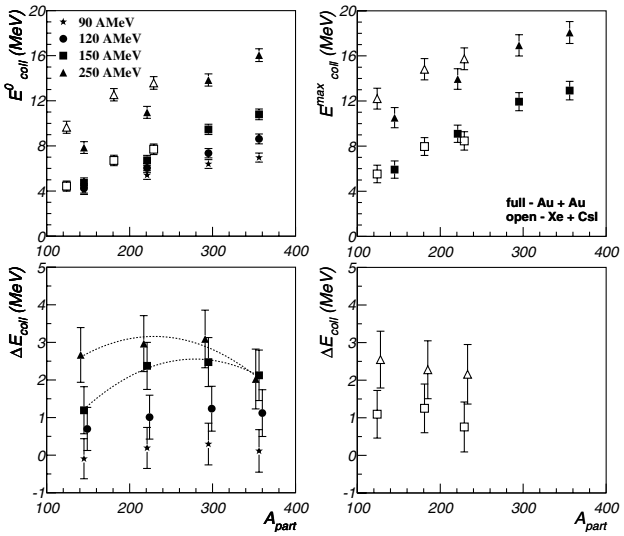

FIG. 2. $E_{\rm coll}^0$ (top-left panel), $E_{\rm coll}^{\rm max}$ (top-right panel), and $\Delta E_{\rm coll}$ (bottom) as a function of $A_{\rm part}$, corresponding to the four centralities mentioned in the text, at different incident energies in the Au + Au (full symbols) and Xe + CsI (open symbols) systems. Second-order polynomial fits, represented by dashed lines, serve to guide the eye.

ΔT in the range 1–2.5 MeV, at 250A MeV. These could be indicative of the small variations of temperatures at the different sides of the participant fireball [7]. Figure 2 provides global results: $E_{\rm coll}^0$, $E_{\rm coll}^{\rm max}$ ($E_{\rm coll}$ at 90°) and $\Delta E_{\rm coll}$ as functions of $A_{\rm part}$ for both measured systems. At 90A MeV, the in-plane and out-of-plane flow values are very similar ($\Delta E_{\rm coll} \sim 0$) at all centralities in Au + Au, paralleling the observations for the yields for which a transition from in-plane to out-of-plane enhancement was found [24] as a function of incident energy. At all energies, $E_{\rm coll}^0$ increases with the centrality corresponding to an increasing baryonic number $A_{\rm part}$ of the fireball. Although the error bars, which include the systematic effects, are large, the relative errors for the data at different $A_{\rm part}$ are small, of the order of 0.08 MeV. At higher energies, a maximum of $\Delta E_{\rm coll}$ in midcentral Au + Au collisions becomes visible. A comparison of the two systems 250A MeV in the 90° direction, outside of the spectator shadow, Fig. 2 (top right), shows a difference of the order of 20% in $E_{\rm coll}^{\rm max}$ between the two systems, at the same $A_{\rm part}$. One should notice that, for the same $A_{\rm part}$, the fireball produced in the Xe + CsI case is more spherical than that in the Au + Au case. This remarkable dependence of the transverse flow energy on the shape of the expanding nuclear zone is reported here for the first time. Flatter fireballs yield on the average less transverse expansion than more spherical ones.

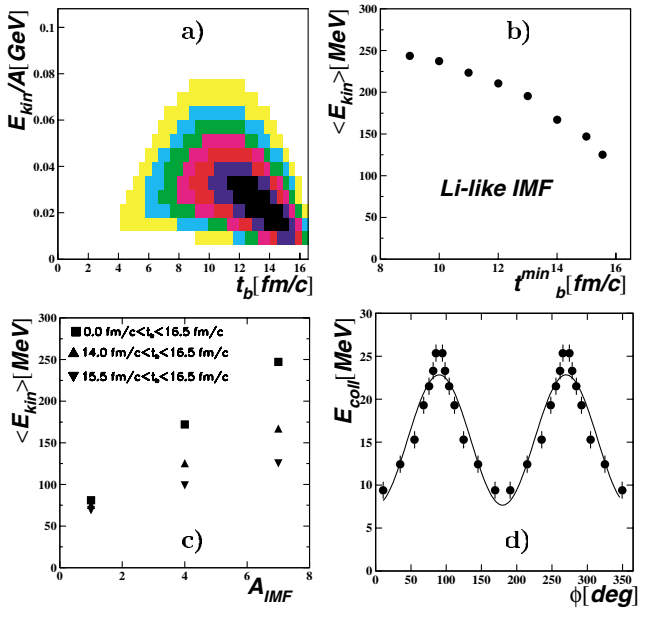

FIG. 3 (color online). (a) Li-like fragment yield distribution in the plane of $E_{\rm kin}$ vs breakup time t_b in the hybrid model. (b) Mean kinetic energy of Li-like fragments emitted after a breakup time $t_b^{\rm min}$. (c) Mean kinetic energy of $Z = 1$, 2, and 3 fragments as a function of their mass for different ranges of the breakup times. (d) Collective energy as a function of azimuthal angle in the hybrid model.

To get an insight on the main mechanism behind the observed experimental trends, we have calculated the expansion dynamics within a semianalytical hybrid model [7] for a 200-nucleon fireball, which roughly corresponds to A_{part} at CM3 centrality in Au + Au collision. Notably, this model, in which expansion dynamics is combined with statistical features of cluster formation at freeze-out, predicts a decrease of the collective energy and of the temperature as the system deexcitation progresses. A two-dimensional yield distribution as a function of E_{kin} and breakup time t_b for Li fragments in 250A MeV Au + Au collision is presented in Fig. 3(a). In the directions outside of the spectator shadow, i.e., perpendicular to the reaction plane, fragments with kinetic energies corresponding to all breakup times will be visible. The situation changes if the observer views the reaction from the reaction plane. Particles emitted directly from the fireball are visible once the spectators moved apart from the collision zone by a distance corresponding to at least half of the transition time. Those particles which were emitted earlier will get redirected. At later times, the E_{kin} distributions become narrower following the decompression and this effect gets more pronounced for heavier fragments. Figure 3(b) shows the mean energy of Li-like fragments as a function of a starting time t_b^{min} for emission, from integrating over the yield in panel 3(a). Mean kinetic energies as a function of fragment mass number A, for different emission intervals in t_b, can be seen in Fig. 3(c). If one calculates the emission in a simple geometric picture, under the assumption that the centers of original nuclei pass each other in the middle of the expansion time shown in Fig. 3(a), one gets the behavior of flow energies represented in Fig. 3(d). Although quite simplistic, the model nicely reproduces the qualitative trends seen in the data, showing that the flow energy values could be viewed as snapshots of the fireball expansion dynamics with different exposure times for different azimuthal directions.

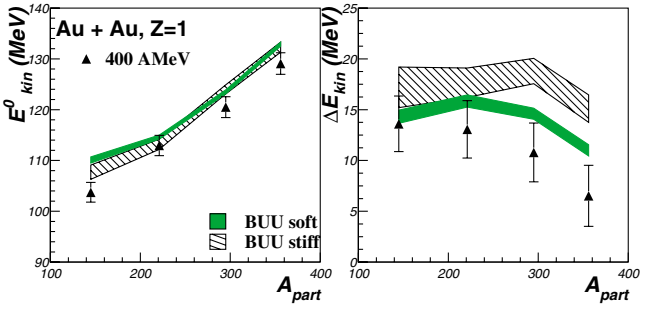

FIG. 4 (color online). E^0_{kin} and ΔE_{kin} as a function of A_{part}, for $Z = 1$ ($A = 1$, 2, 3) fragments, Au + Au at 400A MeV. The experimental results are represented by triangles, while the BUU results are represented by gray zones for soft EOS and by dashed zones for stiff EOS, respectively.

It is obvious that preequilibrium processes can be important and that dynamic long-term anisotropies can be produced in the collective expansion with either effect being absent in the simple scenario above. Thus, a comparison with the *ab initio* microscopic transport model becomes important. Correspondingly, for the 400A MeV Au + Au collisions, we present in Fig. 4 the results of the Boltzmann-Uehling-Uhlenbeck (BUU) transport code [28] using momentum-dependent mean fields ($m^*/m = 0.79$), in-medium elastic cross sections ($\sigma = \sigma_0 \tanh(\sigma^{\mathrm{free}}/\sigma_0)$ with $\sigma_0 = \rho^{-2/3}$), and soft ($K = 210$ MeV, gray zone) or stiff ($K = 380$ MeV, dashed zone) EOS. The light fragments (up to $A = 3$) are produced in a few-nucleon processes inverse to composite breakup. The measured relative yields are nicely reproduced, especially at higher incident energies [8]. The calculated yields have been smeared according to the measured reaction-plane dispersion. For $\langle E_{\mathrm{kin}} \rangle$, little sensitivity to EOS is found, with either EOS parametrization yielding a quite good agreement with the data. As far as the values of ΔE_{kin} are concerned, the calculations with the soft EOS reproduce the overall trend of the experiment while the calculations with the stiff EOS overestimate significantly especially at higher centralities (lower impact parameter) the measured values.

In summary, we presented results on the azimuthal dependence of mean fragment and flow energies in two symmetric systems, for different centralities and incident energies. Corroborated by model estimates, indications emerged that different regions of the azimuth capture different periods of the central fireball expansion. In comparing results from two symmetric systems, it was possible to evidence that a more spherical fireball produces more transverse flow at a given participant number than a deformed fireball. Comparisons with transport code predictions demonstrated that the soft EOS, in combination with a momentum-dependent mean fields and with in-medium cross sections, gives a good agreement with the experiment.

This work was partly supported by the German BMBF under Contract No. RUM-99/010 and No. 06HD953, by the NSF under Grant No. PHY-0245009, and by KRF under Grant No. 2002-015-CS0009.

[1] G. F. Chapline *et al.*, Phys. Rev. D **8**, 4302 (1973).
[2] W. Scheid *et al.*, Phys. Rev. Lett. **32**, 741 (1974).
[3] H.W. Barz *et al.*, Nucl. Phys. **A531**, 453 (1991).
[4] W. Bauer *et al.*, Phys. Rev. C **47**, R1838 (1994).
[5] S. C. Jeong *et al.*, Phys. Rev. Lett. **72**, 3468 (1994).
[6] W. C. Hsi *et al.*, Phys. Rev. Lett. **73**, 3367 (1994.
[7] M. Petrovici *et al.*, Phys. Rev. Lett. **74**, 5001 (1995).
[8] G. Poggi *et al.*, Nucl. Phys. **A586**, 755 (1995).
[9] M. A. Lisa *et al.*, Phys. Rev. Lett. **75**, 2662 (1995).
[10] P. Braun-Munzinger *et al.*, Phys. Lett. B **344**, 43 (1995).
[11] W. Reisdorf *et al.*, Nucl. Phys. **A612**, 493 (1997).

[12] H. Stöcker *et al.*, Phys. Rev. C **25**, 1873 (1982).
[13] H. H. Gutbrod *et al.*, Phys. Lett. B **216**, 267 (1989) .
[14] M. Demoulins *et al.*, Phys. Lett. B **241**, 476 (1990).
[15] D. Brill *et al.*, Phys. Rev. Lett. **71**, 336 (1993).
[16] L. B. Venema *et al.*, Phys. Rev. Lett. **71**, 835 (1993).
[17] Y. Leifels *et al.*, Phys. Rev. Lett. **71**, 963 (1993).
[18] D. Lambrecht *et al.*, Z. Phys. A **350**, 115 (1994).
[19] S. Wang *et al.*, Phys. Rev. Lett. **76**, 3911 (1996).
[20] N. Bastid *et al.*, Nucl. Phys. **A622**, 573 (1997).
[21] Y. Shin *et al.*, Phys. Rev. Lett. **81**, 1576 (1998).
[22] M. Petrovici *et al.*, *Heavy Ion Physics Using* 4π *Detectors* (World Scientific, Singapore, 1997), p. 216.
[23] W. K. Wilson *et al.*, Phys. Rev. C **51**, 3136 (1995).
[24] A. Andronic *et al.*, Nucl. Phys. **A679**, 765 (2001).
[25] J. Ritman *et al.*, Nucl. Phys. **B44**, 708 (1995)
[26] A. Gobbi *et al.*, Nucl. Instrum. Methods Phys. Res., Sect. A **324**, 156 (1993).
[27] P. Danielewicz *et al.*, Phys. Lett. B **157**, 146 (1985).
[28] P. Danielewicz and Q. Pan, Phys. Rev. C **46**, 2002 (1992); P. Danielewicz, Nucl. Phys. **A673**, 375 (2000).